ORIGINAL ARTICLE

Neuroprotective Effect of Chlorogenic Acid in an Animal Model of Sporadic Alzheimer's Disease Induced by Streptozotocin

Jéssica Rabelo Bezerra[1,3] · Tyciane de Souza Nascimento[2,3] · Juliete Tavares[2,3] ·
Mayara Sandrielly Soares de Aguiar[2,3] · Maiara Virgínia Viana Maia[1] · Geanne Matos de Andrade[1,2,3,4]

Abstract

Alzheimer's Disease is a degenerative neurological condition which leads to a decline in memory and cognitive function. Chlorogenic Acid (CGA) presents properties including neuroprotective, antioxidant and anti-inflammatory. The aim of this study was to examine the impact of CGA on cognitive impairments, neuroinflammation and neuronal damage in mice submitted to an experimental model of Sporadic Alzheimer Disease (SAD) induced by intracerebroventricular administration of streptozotocin (ICV-STZ). Male Swiss mice received bilateral ICV-STZ injections (3 mg/Kg) on days 1 and 3. The treatment with CGA (5 mg/Kg, orally) or vehicle (water, orally), was initiated and continued for 26 days, starting 2 h after the second induction procedure. At first, there was no change in serum glucose levels after SAD induction. ICV-STZ induces impairments in aversive, recognition, and spatial memory, while CGA treatment significantly alleviated these memory deficits. Furthermore, locomotor activity, working memory, and anxiety-related activities remained unaffected by the treatments. CGA treatment protects against ICV-STZ-induced increase in the nitrite/nitrate and TBARS levels. ICV-STZ induced a reduction in viable cells, depletion of BDNF, and triggered astrogliosis and microgliosis in the cortex and hippocampus. Treatment with CGA preserves viable cell count in the prefrontal cortex, CA1, and CA3 regions of the hippocampus. Additionally, it prevented BDNF depletion in the prefrontal cortex and hippocampus (CA1, CA3, and DG regions), and mitigated astrogliosis and microgliosis in the prefrontal cortex and hippocampus (CA1, CA3, and DG regions). These findings indicate the neuroprotective effects of CGA, underscoring their potential as therapeutic agents or adjuncts in the treatment of SAD.

Keywords Polyphenol · Dementia · Memory · Neuroprotection · BDNF · Antioxidant

Abbreviations

aCSF	Artificial cerebrospinal fluid
AD	Alzheimer's disease
SAD	Sporadic Alzheimer's disease
ANOVA	Analysis of variance
V	Vehicle
STZ	Streptozotocin
CA	Cornu Ammonis
CGA	Chlorogenic acid
DG	Dentate gyrus, dentate fascia
GFAP	Glial fibrillary acidic protein
Iba-1	Ionized calcium-binding adaptor molecule 1
ICV	Intracerebroventricular route of administration
PBS	Phosphate buffered saline

✉ Geanne Matos de Andrade
gmatos@ufc.br

1 Department of Physiology and Pharmacology, Faculty of Medicine, Federal University of Ceara, Rua Cel. Nunes de Melo 1127, Porangabussu, Fortaleza, Ceará 60430-270, Brazil

2 Department of Clinical Medicine, Faculty of Medicine, Federal University of Ceara, Rua Costa Mendes, Porangabussu, Fortaleza, Ceará 160860430-140, Brazil

3 Laboratory of Neuroscience and Behavior, Drug Research and Development Center (NPDM), , Federal University of Ceará, Rua Coronel Nunes de Melo 1127, Porangabussu, Fortaleza, Ceará 60430-270, Brazil

4 Neuroscience and Behavior Lab, Drug Research and Development Center (NPDM), Federal University of Ceara, Rua Coronel Nunes de Melo, 1000, Fortaleza, CE 60.430-275, Brazil

Introduction

Alzheimer's disease (AD) is a degenerative neurological disorder linked to aging, characterized by the deterioration of memory and gradual cognitive decline [1]. Among the older population, it represents the predominant type of dementia, constituting around 75% of total cases [2]. AD can manifest in two ways: Familial Alzheimer's Disease (FAD) and Sporadic Alzheimer's Disease (SAD), this one that accounts for approximately 95% of AD cases [3, 4]. The pathology of AD constitutes a complex framework involving a combination of genetic, molecular, and environmental factors [5]. AD is characterized by extensive neuronal loss, with the presence of neuritic plaques or senile plaques (NP), which are formed by the extracellular deposition of amyloid-β (Aβ) peptide, intracellular neurofibrillary tangles (NFTs) in the brain, and elevated levels of Aβ (primarily Aβ 40 and Aβ 42) [4, 6].

Also, a series of events lead to neuronal dysfunction, especially in cholinergic neurons, in areas related to cognition and memory formation, such as the prefrontal cortex and the hippocampus, resulting in atrophy in these areas due to neuronal death and cognitive decline [7, 8]. The remaining neurons undergo extensive morphological changes, including neuritic dystrophy, remodeling of axonal trees, and dendritic spine density [9]

Thus, a scenario of neurochemical imbalance is created, characterized by signs of neurodegeneration, neuroinflammation, oxidative stress, increased pro-apoptotic signaling, cholinergic deficits, mitochondrial dysfunction, impairments in synaptic transmission, and disruption of the balance between different neurotransmitters [8, 10]. All of these changes alter the connectivity of memory and cognition circuits, contributing to the symptoms observed in AD [11, 12].

Streptozotocin (STZ) is a naturally occurring glucosamine-nitrosourea that shares a remarkable chemical structure with that of glucose, allowing the drug to be transported into the cell via glucose transporter 2 (GLUT 2) [11, 13]. When administered intracerebroventricularly (ICV), STZ induces a sort of desensitization of insulin receptors and alters the functioning of enzymes involved in cerebral glucose metabolism, leading to biochemical and pathophysiological changes similar to those observed in AD [14] resulting in cognitive deficits [15–18], oxidative stress [19, 20], reduced cerebral glucose metabolism [15], and insulin resistance in the brain [21].

Chlorogenic acid (CGA) is one of the main polyphenols in the human diet, as it is present in tea, coffee, roasted green beans, berries, cocoa, citrus fruits, apples and in many vegetables [22, 23]. Among the various biological activities exhibited by CGA, they include the modulation of glucose metabolism [22, 24], antinociceptive effects [25], antioxidant and anti-apoptotic properties [22], anti-inflammatory action [22], improvement of mood [26], and cognitive function [27, 28].

Moreover, evidence indicates that the consumption of CGA reduces the incidence of different brain diseases such as dementia [4, 29, 30], depression [31], and cerebral ischemia [32]. Furthermore, cellular studies have demonstrated the cytoprotective and neuroprotective effects of CGA [4, 33]. The aim of this study was to investigate the neuroprotective effect of CGA on memory deficits, oxidative stress, cell viability, synaptic plasticity, and neuroinflammatory response induced by ICV-STZ, an experimental model of AD.

Materials and methods

Experimental animals

Adult male albino Swiss mice (25–35 g) from the Central Animal Facility of the Federal University of Ceará (UFC) were used and transferred to the Animal Facility of the Research and Development Center for Drugs of UFC. The animals were housed in appropriate plastic cages, lined with wood shavings, at a temperature of 22 ± 2 °C and a 12 h/12 h light/dark cycle and fed standard food and water ad libitum. All procedures in the study followed the ethical principles of animal experimentation established by the National Council for Animal Experimentation Control (CONCEA). The protocol was approved by the Ethics Committee for Animal Use (CEUA—UFC) of the UFC under registration number 8904290319.

Drugs and chemicals

Streptozotocin and chlorogenic acid were obtained from SIGMA-USA. Ketamine and xylazine were obtained from König (Argentina). All other drugs and reagents utilized were of analytical grade. The artificial cerebrospinal fluid (aCSF), pH 7,4, was compound by NaCl 125 mM, KCl 2.5 mM, NaH_2PO_4 5 mM, $CaCl_2$ 1.2 mM, $MgCl_2$ 1 mM.

Intracerebroventricular (ICV) injection of STZ

The animals were anesthetized with xylazine (10 mg/Kg, i.p.) and ketamine (100 mg/Kg i.p.) and positioned in the precision motorized stereotaxic apparatus with a 10 μm resolution (51730 M, Stoelting, Wood Dale, IL, USA), ensuring proper alignment of the ear bar. To prevent keratitis, the eyes were kept moist with 0.9% saline solution. Skin disinfection was carried out using povidone-iodine (Povidone, Vick Pharma, São Paulo, Brazil). Subsequently, a midline sagittal incision measuring approximately 1.5 cm in length was

made using a scalpel. To validate the correct positioning, the dorsoventral coordinates of bregma and lambda were measured and observed with respect to the flat skull reference.

The openings were created bilaterally on the cranial vault, specifically above the lateral ventricles, employing the following coordinates: 0.5 mm posterior to the bregma, 1.1 mm lateral to the sagittal suture, and 2.8 mm below the brain surface [34]. This particular experimental model of injury was originally introduced by Lannert and Hoyer in 1998 [35]. The perforations were carefully generated on the animal's skull at each designated position using a 1016 FG spherical dental drill affixed to a low-speed Beltec handpiece, LB100, equipped with a high-speed friction adapter chuck, ensuring the preservation of the dura mater and underlying cortex. Any potential bleeding was promptly controlled at this stage. Subsequently, the tip of the Hamilton syringe needle was precisely positioned at the center of each opening. Starting from the initial dorsoventral level of the skull surface at that particular point, the needle tip was gently lowered by 2.8 mm in the dorsoventral direction.

STZ (3 mg/Kg) dissolved in aCSF or aCSF alone (1.5 µL) was bilaterally administered icv in a slow manner (over 1 min) on day 1 and 3 of the experimental timeline, targeting both ventricles and infusing 1.5 µL (45 µg/1.5 µL) of STZ in each hemisphere [36]. To prevent reflux along the syringe, the needle was left in place for an additional 5 min. Following the injections, the incisions made on the animals were closed using 4–0 nylon thread and disinfected with povidone iodine. The animals were allowed to recover from anesthesia on a thermal pad to prevent hypothermia, with the cranial part of their body slightly elevated to avoid airway obstruction. After the administration of STZ-ICV, the animals were divided into four groups (n = 10), as follows: Group I—Artificial cerebrospinal fluid (aCSF) + Vehicle (V), group II—aCSF + CGA, group III—STZ + V and group IV—STZ + CGA.

Chlorogenic Acid (CGA) administration

CGA (5 mg/Kg, p.o.) or vehicle (distilled water) were administered orally (p.o.) as treatment one hour after the induction procedures and continued daily for 25 (twenty-five) days following the second induction procedure [37].

Blood glucose measurement

Glycemia measurements were conducted in all animals without food restriction to confirm non-diabetic status. Measurements were taken immediately prior to the induction procedures and 26 days after ICV-STZ. By employing aseptic surgical scissors, a small blood sample was obtained by puncturing the distal end of the animals' tail. The blood sample was then applied to a test strip for glucose meter reading (On Call® Plus), with results obtained in mg/dL. Mice with fasting glycemia greater than 200 mg/dL and body weight greater than 55 g were classified as diabetic [38].

Behavioral Tests

All behavioral evaluations were performed in a tranquil chamber exclusively designated for behavioral investigations, under low-intensity red light conditions, with controlled temperature and humidity. All apparatus used were made in accordance with specialized literature and were cleaned with 20% ethanol between each animal, except for the Morris water maze. The behavioral examinations were analyzed utilizing the AnyMaze video tracking software (Stoelting Co., Wood Dale, IL, USA). The evaluations were performed in a blinded manner.

Open-Field Test

The locomotor activity and exploratory behavior of the animals were assessed utilizing the open-field apparatus, a black acrylic chamber measuring 30×30 cm, with the floor divided into nine squares of equal size [39]. The animals were placed in the center of the apparatus and allowed to explore the environment freely for a period of 5 min. The parameters measured included total distance covered, average speed, number of quadrants crossed (number of crossings), and number of vertical explorations (rearings), which indicate exploratory behavior where the animals stand only on their hind legs.

Y-Maze Test

In order to evaluate working memory, the spontaneous alternation behavior was evaluated using a three-armed Y-maze ($40 \times 5 \times 16$ cm) positioned at equal angles, following previously established protocols [40]. Prior to the test, the arms were labeled, and the animal was placed at the end of one arm and allowed to alternate entries among the other arms for 8 min. The sequence of arm entries was subsequently recorded and analyzed to determine the number of entries without repetition. The percentage of spontaneous alternation = Alternation behavior × 100/Total number of entries -2, where the alternation behavior is defined as the number of consecutive entries into each of the three arms without repetition.

Novel Object Recognition Test

The novel object recognition task is employed to evaluate recognition memory in mice [41]. This test capitalizes on

the inherent inclination of rodents to explore novel objects within their environment and assesses the mouse's capacity to discriminate between familiar and novel objects. Preceding the test, the mice underwent individual acclimatization in the open field arena for a duration of 5 min, 24 h prior to the test. The experiment took place within the open field arena, with two indistinguishable objects positioned at the corners. The animal was situated in the central quadrant, facing the wall that stood opposite the objects. The test consisted of three sessions. During the initial session, the animal had a 10-min period to explore the open field arena, which contained two identical objects labeled as A and A. In the second session, held one hour later, the object located on the right (A) was substituted with a novel object (B), and the time spent exploring each object (old and new) was measured for 5 min (short-term memory). In the third session, held 24 h later, the familiar object from the first session (A) was substituted with a novel object (C), and the time spent exploring each object (old and new) was measured for 5 min (long-term memory). The recognition or discrimination index was computed using the following formula: (time spent exploring the new object—time spent exploring the familiar object) divided by (time spent exploring the new object + time spent exploring the familiar object). The following actions were considered as object exploration: sniffing, licking, or touching the object with the nose or front paws, or directing the nose towards the object at a distance of ≤ 1 cm.

Passive Avoidance Test

The passive avoidance test enables the evaluation of short and long-term memories, as well as aversive memory, utilizing the animal's natural inclination to explore beyond the platform [42]. The animals were acclimatized to the passive avoidance device (Insight LTDA), which comprises an acrylic box ($48 \times 22 \times 22$ cm) with an electrified floor and a non-electrified platform. The animal was placed on the platform for 1 min to acclimate to the apparatus and then removed. After 30 s, the animal was placed back on the platform. Since the animal tends to explore its surroundings, it receives a 0.5 mA shock for 1 s when it descends from the platform, with the latency time to descend being recorded for up to a maximum of 5 min (training). Animals that did not descend from the platform were shocked after 5 min of training. After 15 min, the animal was removed and placed back on the platform (early memory). Learning retention was assessed after 24 h (late memory) without the animals receiving any shocks at this stage.

Morris Water Maze Test (MWM)

In this version of the water maze task, which was previously described by Morris [43], mice acquire the ability to swim towards a submerged platform as quickly and efficiently as possible. Clues present in the room walls and other external visual stimuli guide the animals, to evaluate visuospatial learning and memory (long-term). The successful completion of this task relies on proper functioning of the hippocampus.

This apparatus comprises a large circular pool filled with opaque water, in which a platform is situated just below the water surface, hidden from the view of the rodent. Each animal was randomly placed into the circular pool (90 cm in diameter and 60 cm deep) filled with turbid water (up to 30 cm high) tinted with non-toxic black ink at 26 °C. The pool was spatially divided into four quadrants, with a submerged platform (7 cm in diameter) positioned 2 cm below the water surface, where the animal had 60 s to locate the platform and remain there for 10 s. The training entailed six sessions per day for two consecutive days, during which the animal underwent learning, with 30-s intervals between each training session. Following 48 h after the last training session, the animal was subjected to the test without the platform to assess memory acquisition. During the test, the animal was placed in the pool for 60 s, and the duration of time it remained in the quadrant where the platform was previously located, the latency period to locate the platform, and the number of times it crossed the exact location of the platform were documented.

Estimation of Brain Thiobarbituric Acid Reactive Species (TBARS) Level

The antioxidant activity was measured by assessing the levels of thiobarbituric acid reactive substances (TBARS) [44], an indicator of lipid peroxidation. For the assay, 60 μL of the cortex and hippocampus homogenate (10% in phosphate buffer) was added to a test tube and centrifuged at 1,200 rotations per minute (rpm) at 4ºC for 30 min. After centrifugation, 100 μL of 35% perchloric acid was added to stop the peroxidation, and centrifuged again at 5,000 rpm at 4 °C for 10 min. The supernatant was collected and 50 μl of 1.2% thiobarbituric acid was added. Subsequently, the solution was placed in a water bath for 30 min at a variable temperature of 95–100 °C. The solution was removed and allowed to cool to room temperature. After cooling, 150 μL of the solution was added to the wells of the ELISA plate and read at 535 nm. Malondialdehyde (MDA) is the end product of lipid peroxidation and reacts with TBARS, so the standard curve was obtained by reading several concentrations (640, 320, 160, 80, 40, 20, 10, 5, 2.5, 1.2, 0.6 μM) of standard MDA, and the results were expressed in concentration (μM).

Determination of Nitrite/Nitrate Concentration

In this assay, the Griess reagent (0.1% N-1-naphthyleth-ylenediamine in distilled water, 1% sulfanilamide in 5% phosphoric acid, in a 1:1 ratio) reveals the presence of nitrite/nitrate (NO_2/NO_3) in a sample through a diazotiza-tion reaction that forms a pink-colored chromophore, with a peak absorbance at 540 nm [45]. For the assay, cortical and hippocampal homogenates (10% in phosphate buffer) were centrifuged at 1,200 rpm for 15 min at 4 °C, and 100 μL of each supernatant was added to 100 μL of the Griess reagent. For the blank, 100 μL of phosphate buffer and 100 μL of the Griess reagent were used. After 10 min, the absorbances were read at 540 nm. The standard curve was obtained by reading various concentrations of standard nitrite (100; 50; 25; 12.5; 6.52; 3.12; 1.56; 0.78; 0.39; 0.195 μM) and the results were expressed in concentra-tion (μM). The absorbance readings of the standards (y) were plotted against the concentration of each standard (x), and then the equation of the line was determined, which was used to determine the nitrite concentration in each sample.

Cell Viability Evaluation

Twenty-eight days after ICV-STZ and behavioral tests, the animals were perfused through the heart, with saline (8º-10ºC), followed by 4% paraformaldehyde in PBS. The brains were post-fixed in buffered formalin for 24 h, and were stored at -20ºC in 30% in sucrose solution. The tissue was cut in the cryostat (10 μm) and the slices were mounted on silanized glass slides representative of the prefrontal cor-tex (PFC) and hippocampus. The tissues were then stained using the Cresyl Violet technique to verify neuronal viabil-ity [46, 47]. The brain slice slides of the prefrontal cor-tex and hippocampus were immersed in distilled water for one minute, and subsequently incubated in a 0.5% cresyl violet solution prepared in acetate buffer (20% sodium acetate 2.7% + 80% 1.2% glacial acetic acid) for a period of three minutes. The marking was fixed with two washes in the acetate buffer. Then, the slides were dehydrated in alcohol (50, 70, and 100%). Finally, they were immersed in xylene and mounted with Entellan (Merck, Germany). For the quantification of Nissl-stained neurons, the slides were viewed under a microscope (Nikon Eclipse E200) at a $200 \times$ magnification. Three slices from each animal were randomly selected, and three areas in each slice were ana-lyzed. The quantification of stained neurons was performed on all images using Image J software (NIH, Bethesda, MD, USA) with a 1000-grid. In the hippocampus, the subfields CA1, CA3, and DG (Dentate Gyrus) were analyzed. The mean of the three values per animal was calculated, and the results were expressed as the number of viable cells.

Cells were considered viable neurons when they showed violet staining in the cytoplasm, as well as normal morpho-logical features (round or oval-shaped cells with centralized nuclei).

Immunohistochemistry for BDNF, GFAP and Iba-1

The prefrontal cortex and hippocampus slices (10 μm thick-ness) were washed three times for 5 min in PBS. Endoge-nous peroxidase blocking was performed with 1.05% H_2O_2 in 10% methanol in PBS for 40 min at room temperature. After this step, the slices were washed three times for 5 min in PBS and endogenous protein blocking was performed with a blocking solution (10% horse serum and 1% Triton X-100 in PBS) for 2 h at room temperature. Then, the slices were incubated in primary antibodies diluted in PBS with 0.25% Triton-X100 and 5% horse serum for 48 h: primary antibody anti-BDNF (1:200, Sigma); primary antibody anti-GFAP (rabbit, 1:200, Sigma); and primary antibody anti-iba-1 diluted in blocking solution (rabbit polyclonal, 1:300; WAKO, Japan) overnight at 4 °C.The slices were then washed 3 times for 10 min in PBS, and subsequently incubated with HRP-conjugated mouse and rabbit anti-body (1:300) linked polymer (Dako EnVision + Dual Link System-HRP, Dako) for 2 h at room temperature (RT), and washed again 3 times for 5 min with PBS. The staining was revealed with 3,3'-diaminobenzidine (DAB Peroxidase Substrate Kit; Dako). The reaction was stopped by washing the slides in distilled water, after drying the slides were immersed in xylene and mounted with entellan (Merck, Germany).

For immunoreactivity quantification, the slides were visualized under a microscope (Nikon Elipse E200) at $100 \times$ magnification. Three slices from each animal and three areas within each slice were randomly selected, and semi-quantitative quantification of optical density was performed on all images using Image J software (NIH, Bethesda, MD, USA). The final optical density of each image was obtained by subtracting the density of the white background from the density of the total image. The mean of the three values per animal was calculated, and the mean of the values obtained for the control group was also calculated, with the remaining values expressed as a percentage of that value.

Statistical Analysis

Statistical analyses were performed using GraphPad Prism 6.01 software (GraphPad Software, Inc.), and all data are expressed as mean ± SEM. The normality of the data dis-tribution was assessed initially using the D'Agostino and Pearson normality test and the Shapiro–Wilk normality test. For data with a normal distribution, one-way analysis of variance (ANOVA) followed by the Bonferroni post-hoc test

Table 1 Effect of ICV-STZ and CGA on blood glucose levels

Blood glucose levels (mg/dL)		
Groups	d0	d29
aCSF + V	115.8 ± 5.715	111.0 ± 3.765
aCSF + CGA	120.2 ± 3.630	110.2 ± 2.598
STZ + V	123.6 ± 7.755	116.6 ± 6.327
STZ + CGA	119.7 ± 4.467	117.6 ± 5.239

The animals were treated with CGA orally for 26 days. The analysis of blood glucose levels in mice (n = 10 animals/group) was conducted on days 0 and 29, prior to the induction procedures and immediately before euthanasia of the animals, using blood glucose strips. Values are presented as mean ± SEM. aCSF (artificial cerebrospinal fluid); V (Vehicle—distilled water, oral); STZ (Streptozotocin); CGA (Chlorogenic Acid)

was employed. A significance level of $p < 0.05$ was considered for all tests.

Results

Peripheral Blood Glucose Levels in Mice

The results obtained from the peripheral blood glucose levels demonstrated no significant alterations before and after the induction procedures with STZ, and with the treatment of CGA, indicating that the animals did not develop diabetes (Table 1).

Effect of CGA on Locomotor Activity of Mice with SAD by ICV-STZ

The results obtained from the open field test demonstrated that there were no significant changes between the groups in relation to the distance covered (Fig. 1A), average speed (Fig. 2B), and the number of crossings and rearings (Fig. 1C).

Effect of CGA on Memory of Mice with SAD Induced by ICV-STZ

In the assessment of working memory using the Y-maze test, no significant changes were observed between the groups (Fig. 2A).

In the evaluation of the recognition index using the novel object recognition test, animals subjected to ICV-STZ showed deficits in the ability to recognize a new object during the exposure after 1 h ($p < 0.01$, Fig. 2B) and 24 h ($p < 0.01$, Fig. 2C) compared to animals in the aCSF group. Treatment with CGA protected against memory deficit in
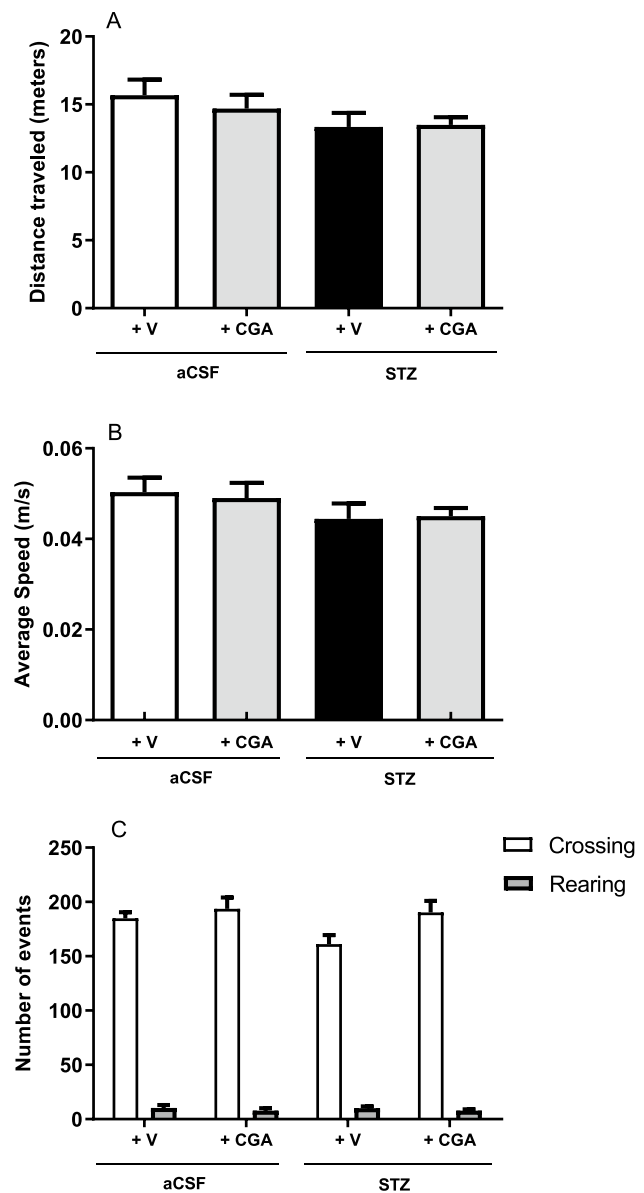
Fig. 1 The CGA does not alter the locomotor activity of animals with SAD induced by ICV-STZ. The animals were treated with CGA for 26 days, and the distance covered (**A**), average speed (**B**), and the number of crossings and rearings (**C**) were evaluated using the ANYmaze software (Stoelting Co., USA) for 5 min, 12 days after ICV-STZ. Values are presented as mean ± SEM (n = 10 animals/group). aCSF (artificial cerebrospinal fluid); V (Vehicle—distilled water, oral); STZ (Streptozotocin); CGA (Chlorogenic Acid)

the object recognition test after 1 h ($p < 0.05$, Fig. 2B) and 24 h ($p < 0.05$, Fig. 2A).

In the evaluation of aversive memory, the animals subjected to ICV-STZ showed deficits in the retention of early memory (EM) (latency (s), $p < 0.05$) and late memory (LM) (latency (s), $p < 0.0001$) when compared to animals in the aCSF group (Fig. 2D). This deficit was attenuated by
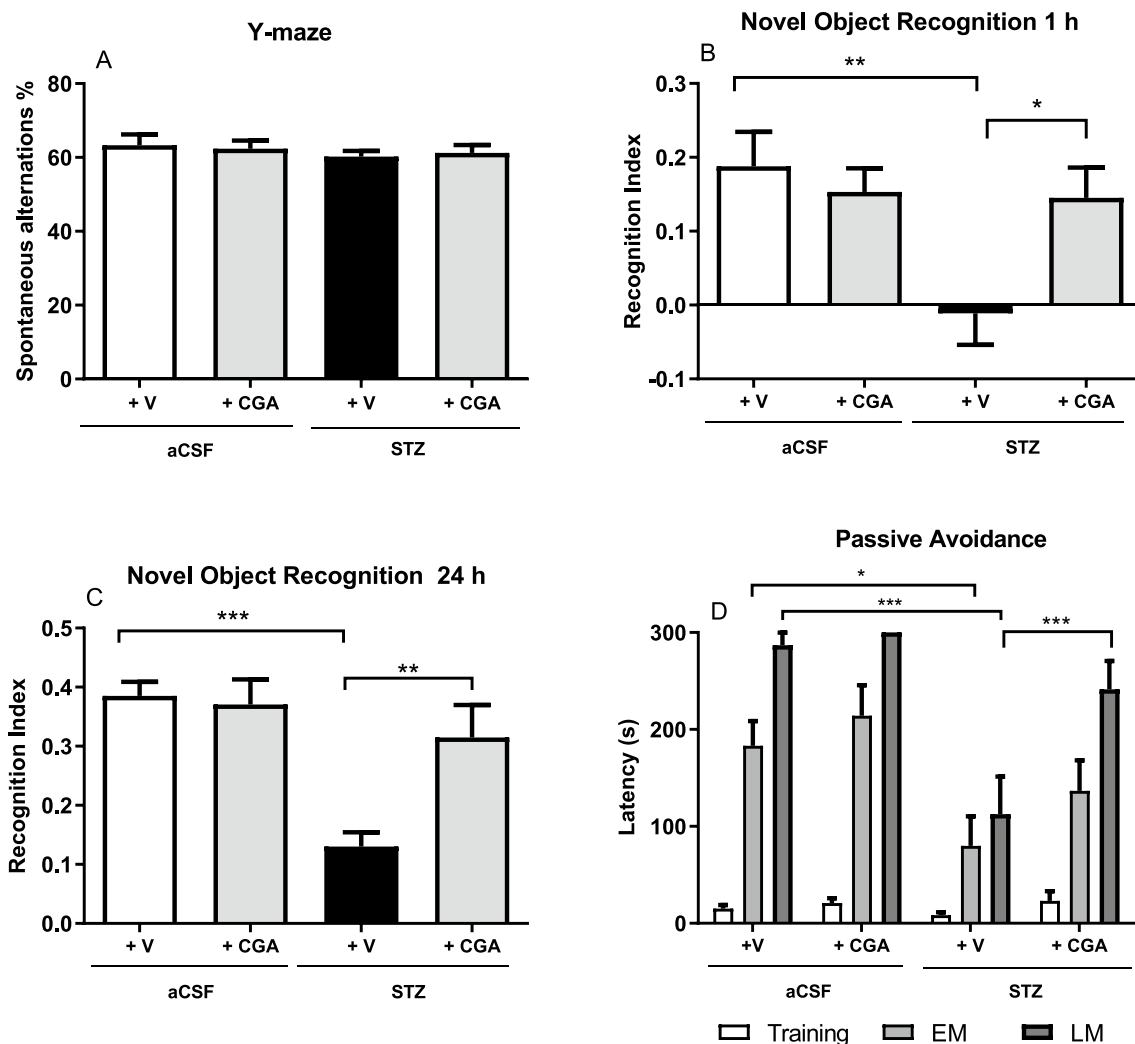
Fig. 2 Effect of CGA treatment in the working memory (**A-C**) and aversive memory (**D**) of animals with SAD induced by ICV-STZ. For Y-maze (**A**), the animals were treated with CGA for 26 days, and the number of spontaneous alternations was counted during an 8-min at day 22 days after ICV-STZ. The recognition index was analyzed 23 days after the ICV-STZ, 1-h (**B**) and 24 (**C**) hours after the presentation of the objects, and the latency time for the animals to descend from the platform (**D**) was measured during 300 s, conducted at 15 min (early memory—EM) and 24 h (late memory—LM) after training, on days 24 and 25, respectively. Values are presented as mean ± SEM. *$p<0.05$; **$p<0.001$ and $p<0.0001$, One-way ANOVA followed by the Bonferroni test (n = 10 animals/group). aCSF (artificial cerebrospinal fluid); V (Vehicle—distilled water, oral); STZ (Streptozotocin); CGA (Chlorogenic Acid)

CGA treatment in late memory (LM) (latency (s), $p<0.01$) (Fig. 2D).

Effect of CGA on Spatial Memory Deficit of Mice with SAD Induced by ICV-STZ

In the evaluation of spatial memory through the water maze, animals submitted to ICV-STZ showed deficits in memory, presenting a longer latency time to find the platform when compared to animals in the aCSF group (latency (s), $p<0.05$). The treatment with CGA significantly decreased the latency time to find the platform location (latency (s), $p<0.05$) (Fig. 3A, G). The mice subjected to ICV-STZ exhibited a decrease in time spent in the quadrant ($p<0.05$). The treatment with CGA resulted in a significant increase in the time spent in the quadrant ($p<0.05$) (Fig. 3B). Regarding the number of crossings at the platform site, animals subjected to ICV-STZ exhibited a reduction in the number of crossings ($p<0.05$). Treatment with CGA was able to increase the number of crossings at the platform site ($p<0.05$) (Fig. 3C). The animals that received ICV-STZ presented a decrease in the number of crossings ($p<0.05$), CGA was effective in increasing the number of entries in the quadrant where the platform was located ($p<0.05$) (Fig. 3D). There were no statistical differences between the groups regarding the distance

Fig. 3 The CGA protected against spatial memory deficits of animals with SAD induced by ICV-STZ. The animals were treated with CGA (5 mg/Kg, p.o.) for 26 days after ICV-STZ, and the latency (**A**), time in quadrant (**B**), the number of crossings on the platform (**C**), entries in the quadrant (**D**), average speed (**E**), average speed (**F**), was evaluated by the ANYmaze software (Stoelting Co., USA) during 1 min, G- Illustrative image of the animal's trajectory to the platform location. The results are presented as mean ± SEM. $*p < 0.05$; $**p < 0.005$; $***p < 0.0001$, One-way ANOVA, followed by the Bonferroni Test (n = 10 animals/group). aCSF (artificial cerebrospinal fluid); V (Vehicle—distilled water, p.o.); STZ (Streptozotocin); CGA (Chlorogenic Acid)
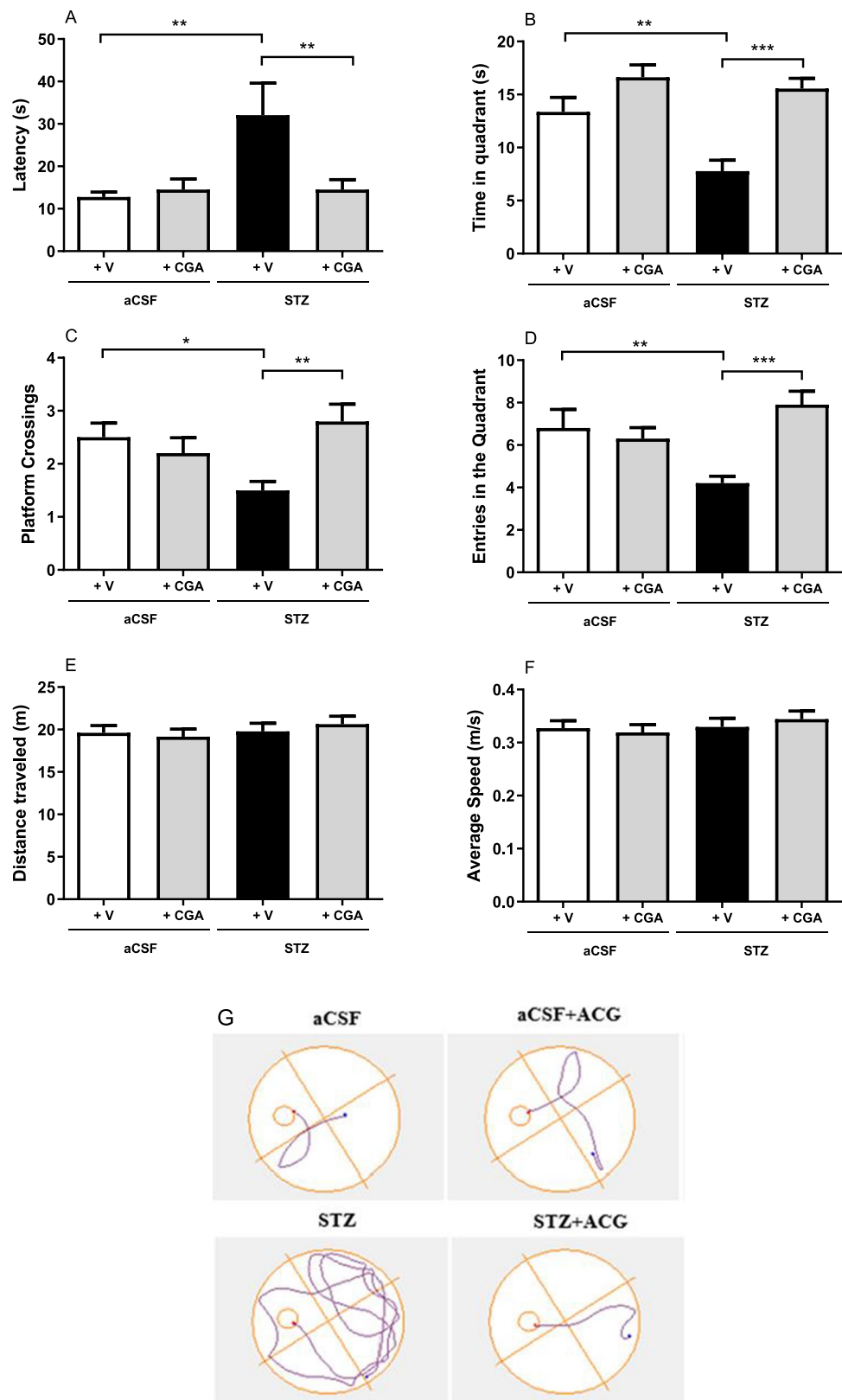
covered by the animals until they reached the platform or the average speed (Fig. 3E, F).

Effect of CGA on Nitrite/Nitrate (NO_2/NO_3) and TBARS Levels of Mice with SAD Induced by ICV-STZ

In the assessment of nitrite/nitrate levels in the cortex and hippocampus, animals subjected to STZ injections exhibited a significant increase in nitrite concentrations in cortex ($p < 0.05$), and hippocampus ($p < 0.05$). Treatment with CGA was able to protected against the increase in nitrite concentration in both brain regions, (Fig. 4A), and in the hippocampus (Fig. 4B).

The animals subjected to STZ injections showed a significant increase in TBARS concentrations in cortex ($p < 0.05$), and hippocampus ($p < 0.05$). Treatment with CGA was able to protect against the increase in TBARS concentration in both brain regions (cortex: $p < 0.05$, (Fig. 4C), and hippocampus ($p < 0.05$, Fig. 4D).

Effects of CGA on Neuronal Viability in the Prefrontal Cortex and *Hippocampus* of Mice with SAD Induced by ICV-STZ

A decrease in cell viability was observed in the prefrontal cortex (Fig. 5) and hippocampus (CA1, CA3 regions)

(Fig. 5) of animals subjected to ICV-STZ. The treatment with CGA protected against the decrease in the number of viable cells in all regions studied, except in DG region (Fig. 5).

Effects of CGA on BDNF Immunoreactivity in the Prefrontal Cortex, and *Hippocampus* of Mice with SAD Induced by ICV-STZ

A decrease in BDNF immunoreactivity was observed in the prefrontal cortex and hippocampus (CA1, CA3 and DG) of mice with SAD by ICV-STZ. The CGA prevented this decrease in all regions studied (Fig. 6).

Effects of CGA on Astrocyte Activation Assessed through Immunostaining with GFAP in the Prefrontal Cortex and *Hippocampus* of Mice with SAD Induced by ICV-STZ

The evaluation of astrogliosis through immunostaining with GFAP revealed an increase in astrocyte activation in the prefrontal cortex and hippocampus of animals subjected to STZ injections. Treatment with CGA significantly reduced astrocyte activation in both areas studied (Fig. 7).
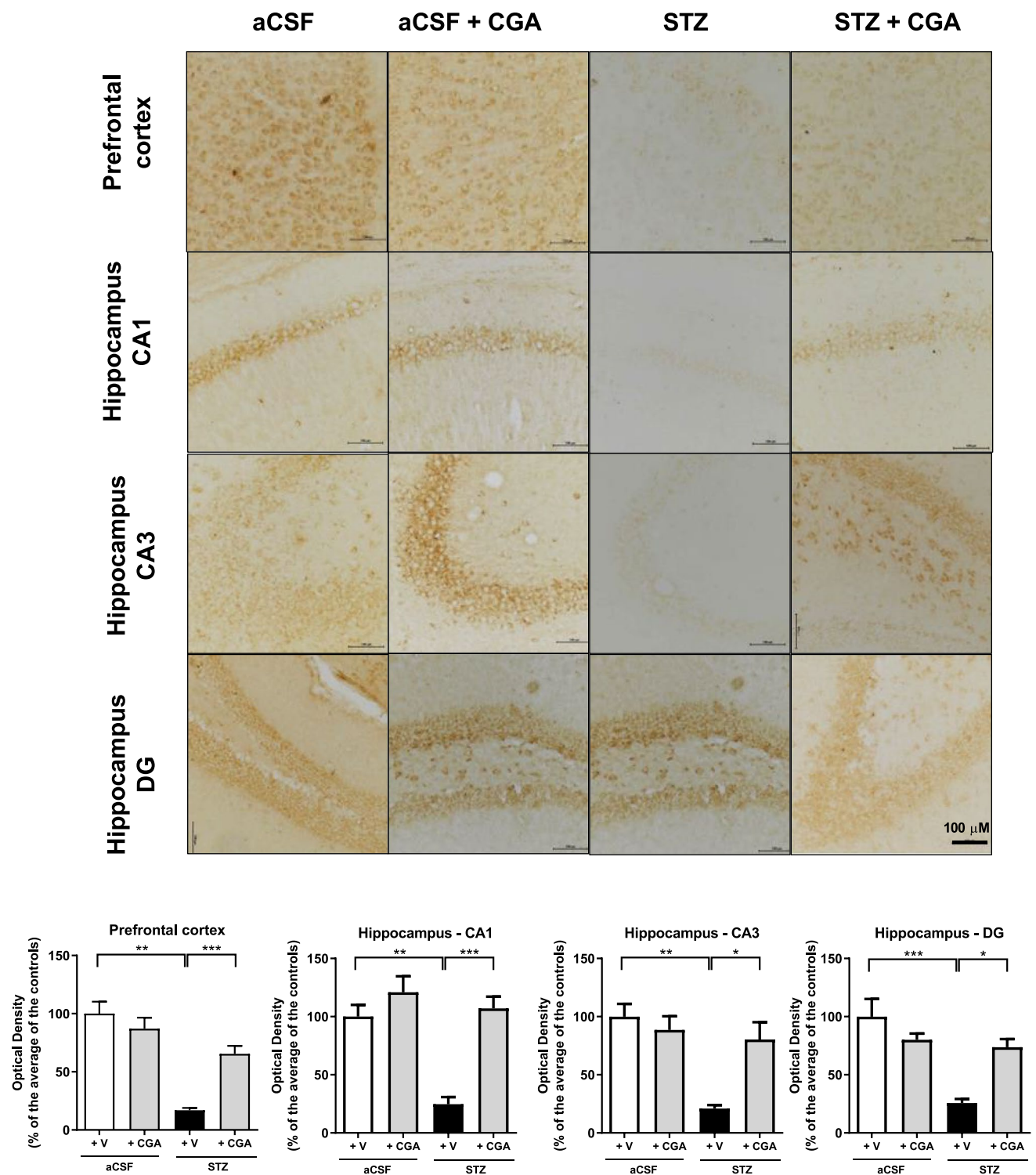

Fig. 4 The CGA decreased nitrite/nitrate levels in the cortex and hippocampus of mice with SAD induced by ICV-STZ. The animals were treated with CGA for 26 days after ICV-STZ, and the dissected areas were used for nitrite/nitrate and TBARS measurement. The results are presented as mean ± SEM. *$p < 0.05$; **$p < 0.005$; ***$p < 0.0001$. One-way ANOVA followed by the Bonferroni Test (n = 6/group). aCSF (artificial Cerebrospinal Fluid); V (Vehicle—distilled water, p.o.); STZ (Streptozotocin); CGA (Chlorogenic Acid)
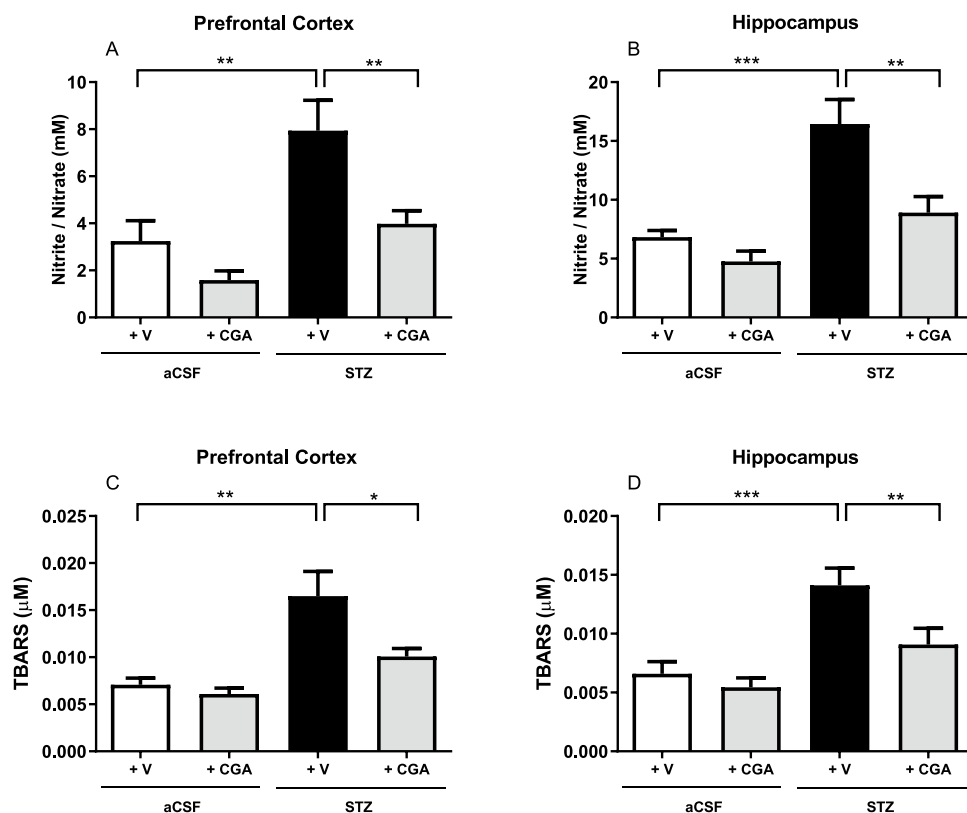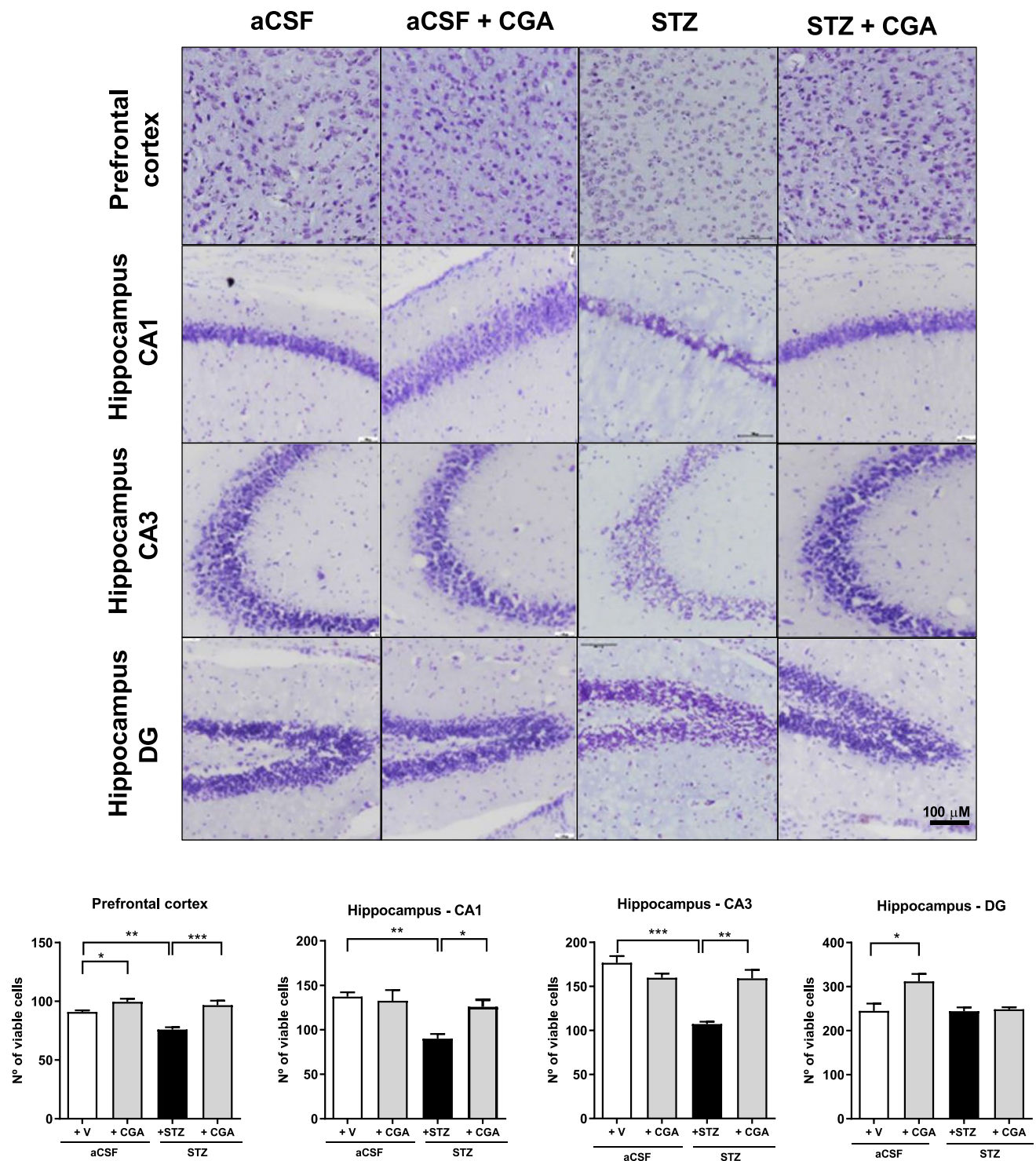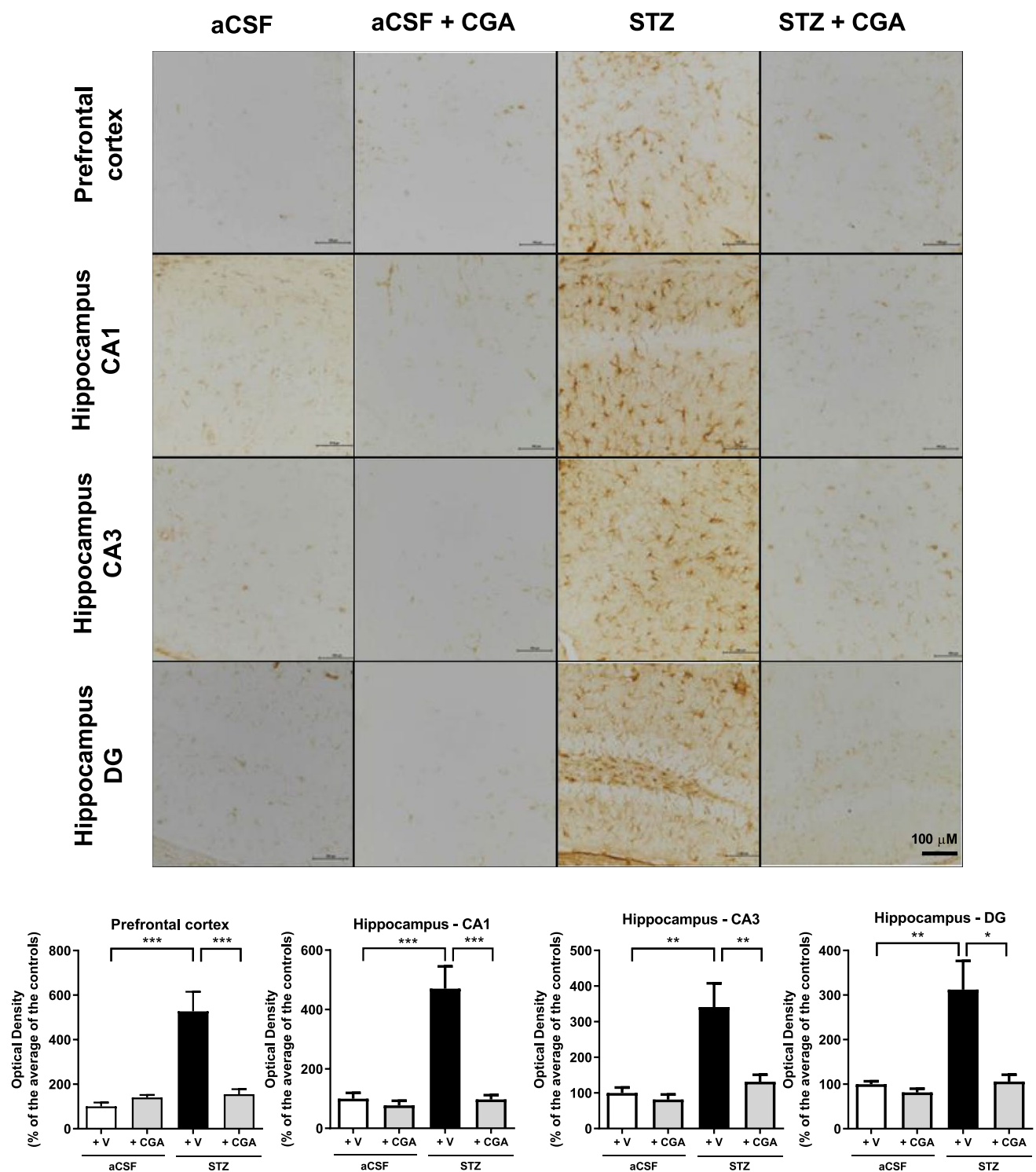
Fig. 5 The CGA protected against decreased on neuronal viability in prefrontal cortex and hippocampus of mice with SAD induced by ICV-STZ. The animals were treated with CGA for 26 days, and the brains were perfused for histological analysis with Cresyl Violet 26 days after ICV-STZ. **A)** Photomicrographs representative of the effect of CGA on cell viability in the prefrontal cortex, and hippocampus (CA1, CA3, and DG regions). **B)** The results are presented as mean $\pm$ SEM. $*p < 0.05$; $**p < 0.005$; $***p < 0.0001$, One-way ANOVA followed by the Bonferroni Test ($n = 5$–6 animals/group, 3 slices/animal). aCSF (artificial Cerebrospinal Fluid); V (Vehicle—distilled water, oral); STZ (Streptozotocin); CGA (Chlorogenic Acid). Visualization: Nikon Elipse E200 microscope, $200 \times$ magnification, scale bar of 100 μm

Fig. 6 The CGA increased BDNF immunoreactivity in the cortex and hippocampus of mice with SAD induced by ICV-STZ. The animals were treated with CGA for 26 days, and the brains were perfused for assessment of BDNF immunoreactivity after ICV-STZ. **A)** Photomicrographs representative for BDNF immunoreactivity in the prefrontal cortex, and hippocampus (CA1, CA3, and DG regions).

B) The results are presented as mean $\pm$ SEM. $*p < 0.05$; $**p < 0.005$; $***p < 0.0001$. One-way ANOVA followed by the Bonferroni Test (n $=$ 5–6 animals/group, 3 slices/animal). aCSF (artificial Cerebrospinal Fluid); V (Vehicle—distilled water, oral); STZ (Streptozotocin); CGA (Chlorogenic Acid). Visualization: Nikon Elipse E200 microscope, 200 $\times$ magnification, scale bar of 100 μm

Fig. 7 The CGA decreased GFAP immunoreactivity in the cortex and hippocampus of mice with SAD induced by ICV-STZ. The animals were treated with CGA for 26 days, and their brains were perfused for GFAP immunoreactivity 26 days after ICV-STZ. **A)** Photomicrographs representative of GFAP immunoreactivity in the prefrontal cortex, and hippocampus (CA1, CA3, and DG regions).

B) The results are presented as mean $\pm$ SEM. $*p < 0.05$; $**p < 0.005$; $***p < 0.0001$. One-way ANOVA followed by the Bonferroni Test (n = 5–6 animals/group, 3 slices/animal). aCSF (artificial cerebrospinal fluid); V (Vehicle—distilled water, orally); STZ (Streptozotocin); CGA (Chlorogenic Acid). Visualization: Nikon Eclipse E200 microscope, 200×magnification, scale bar of 100 µm

Effect of Chlorogenic Acid on Microglial Activation through iba-1 Immunostaining in the Prefrontal Cortex and *Hippocampus* of Mice with SAD Induced by ICV-STZ

In the evaluation of microgliosis, through iba-1 immunostaining, an increase in microglial activation was observed in the prefrontal cortex and hippocampus of animals subjected to ICV-STZ. Treatment with CGA significantly decreased microglial activation in both areas studied (Fig. 8).

Discussion

In this study, the neuroprotective potential of CGA was demonstrated in relation to cognitive deficits, reduction in neuronal viability, decrease in BDNF expression, and increased oxidative stress and neuroinflammation in mice subjected to the ICV-STZ-induced SAD model. AD is a neurological disorder that is still poorly understood, and its multiple pathological pathways contribute to the complexity and difficulty in treating and preventing this disease. Since there is currently no cure for AD, the main challenge lies in the development of new therapies and/or therapeutic targets for curing or providing symptomatic treatment for the disease [1–5].

The model used in this study, the ICV-STZ-induced SAD model, causes desensitization of insulin receptors (IR), thereby altering the functioning of enzymes involved in among them due to its anti-inflammatory and antioxidant activity and for inhibiting the activity of acetylcholinesterase, increasing the supply of acetylcholine in the synaptic cleft and improving brain glucose metabolism. This leads to biochemical and pathophysiological changes similar to those observed in AD [14] including oxidative stress, neuroinflammation, neuronal loss, and impaired learning and memory [16–18]. To exclude the potential effects of STZ in altering glucose metabolism at the systemic level, blood glucose levels were measured. It has been demonstrated that ICV-STZ does not alter blood glucose which remained below 200 mg/dL, the average blood glucose level used as a basis for classifying a diabetic animal. This data is in accordance with other studies whit demonstrated that STZ is not able to penetrate blood–brain barrier which lacks GLUT2 transporter [11, 47].

In a second step, we evaluated the behavioral changes, first locomotor activity followed by changes in memory and cognition, induced by the SAD model as well as the protective potential of CGA. So, it was demonstrated that there were no changes in terms of distance traveled, average speed, and the number of crossings and rearings in the open-field test. These data support studies that show no alteration in locomotor activity and exploratory behavior in animals that received ICV-STZ, ruling out the possibility of STZ interfering with locomotor activity in memory tests (Pacheco et al., 2018) and indicating no motor deficit in the animal model of SAD. Additionally, treatment with CGA also did not alter the locomotor activity of the animals, as previously shown by Fernandes et al. [48].

Animals that received ICV-STZ showed a deficit in object recognition memory, corroborating data from the literature [49]. The difficulty in memory acquisition and retention in this model is probably associated with impaired brain insulin signaling in the hippocampus [50]. Treatment with CGA was able to promote a significant improvement in the object recognition index after exposure at 1 h and 24 h. In the evaluation of aversive memory, the animals submitted to the SAD model showed deficits in early and late memory, corroborating previous data in the literature [49, 51], and CGA treatment also protected against deficits in delayed aversive memory. Studies by Kwon et al. (2010) corroborate our findings, they showed an improvement in aversive memory after treatment with CGA in the model of amnesia induced by scopolamine, a muscarinic antagonist, for inhibiting acetylcholinesterase activity. Lee et al. [34] showed an improvement in aversive memory after treatment with CGA in a transient brain ischemia model, and this protective effect was possibly due to its anti-inflammatory and antioxidant activity.

After the behavioral tests, neurochemical parameters were investigated. First we investigated the redox status since oxidative stress has been associated with the onset and progression of AD [52, 53] because it can induce membrane lipid damage, changes in enzymes critical to neuronal and glial function, and structural DNA damage. These effects lead to tissue damage, synapse dysfunction, and cell death [54]. Studies have shown that ICV-STZ causes memory impairment in rodents through increased oxidative stress, which is associated with chronic neuroinflammation, neuronal damage, apoptosis, and ultimately neurodegeneration [55, 56]. Another contributing factor to oxidative stress is the malfunctioning of the IR on ICV-STZ, which also results in a reduction in cerebral energy metabolism. This reduction leads to the accumulation of reactive species followed by oxidative stress, which is reflected in cognitive dysfunctions. One of the contributing factors to these dysfunctions is the inhibition of ATP and acetyl-CoA formation [57]. Treatment with CGA protected against increased nitrite and TBARS concentration in the cortex and hippocampus, demonstrating that the antioxidant effect of CGA may be involved in its neuroprotective effect against oxidative damage induced by ICV-STZ. Like most polyphenols, CGA has been described as a potent antioxidant [28], and several studies have shown the ability of CGA to affect brain function by combating free radical formation and decreasing neuronal death [29, 30, 58, 59]. Furthermore, it has been discovered that the
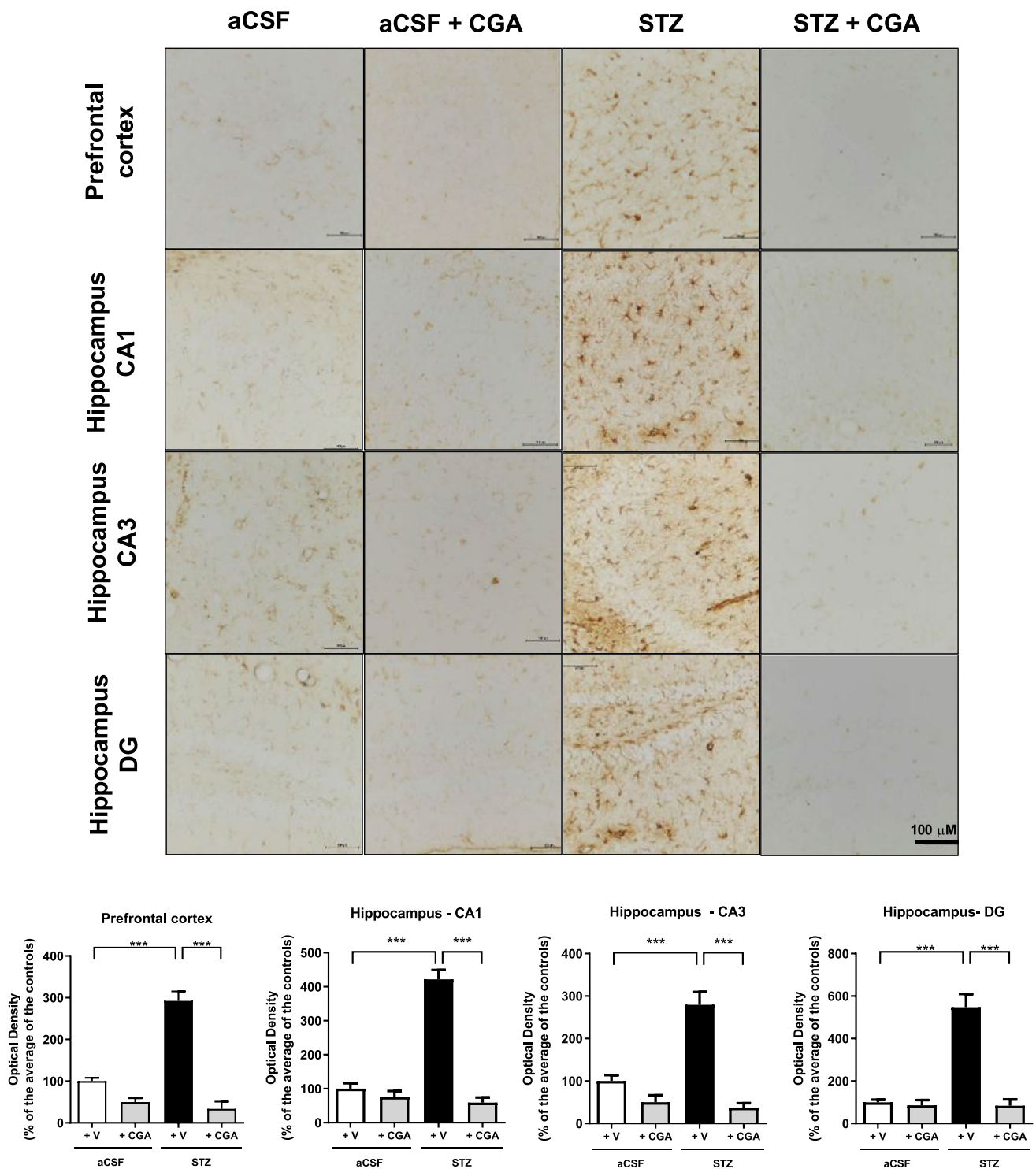
Fig. 8 The CGA decreased iba-1 immunoreactivity in the cortex and hippocampus of mice with SAD induced by ICV-STZ. The animals were treated with CGA for 26 days, and their brains were perfused for iba-1 immunoreactivity 26 days after ICV-STZ. **A)** Photomicrographs representative of iba-1 immunoreactivity in the prefrontal cortex, and hippocampus (CA1, CA3, and DG regions). **B)** The results are presented as mean ± SEM. $*p < 0.05$; $**p < 0.005$; $***p < 0.0001$. One-way ANOVA followed by the Bonferroni Test (n = 5–6 animals/group, 3 slices/animal). aCSF (artificial cerebrospinal fluid); V (Vehicle—distilled water, oral); STZ (Streptozotocin); CGA (Chlorogenic Acid). Visualization: Nikon Elipse E200 microscope, 200 × magnification, scale bar of 100 μm

hydroxyl groups in its structure act as positive moieties for its antioxidant properties [60].

Many studies have already shown a reduction in cell viability, especially due to the the presence of extracellular amyloid plaques composed of the Aβ peptide [61]. Inhibition of oligomerization and prevention of Aβ-induced cell death are potential targets for the development of AD therapies [62, 63]. The Aβ peptide is also associated with neuronal apoptosis in AD [64]. Studies have shown that pathological changes in the STZ-induced AD model occur in different phases, including an acute phase (1 to 3 months), a compensatory phase (6 to 9 months), and a decompensatory phase, with a progressive decline in the chronic phase [65]. Studies using the ICV-STZ SAD model indicate that Aβ plaque formation occurs after a minimum of 3 months of ICV-STZ injections [20]. However, evidence shows a significant increase in Aβ protein expression in the hippocampus at 14 days after STZ administration, decreasing on day 21 [66]. This suggests that the accumulation of Aβ plaques in the hippocampus may be related to cell death, followed by the decline in cognitive function characteristic of SAD [1]. STZ, like other alkylating agents in the nitrosourea class, is toxic to cells because it forms carbonium ions which cause damage by DNA methylation [67]. These findings corroborate the reduction in cell viability and cognitive deficits STZ-induced demonstrated in this study. We demonstrate decreased neuronal loss in the cortex and hippocampus with CGA treatment, other authors related the cognitive effect of CGA to the decrease neuronal losses in the hippocampus, decrease autophagy, and improve synaptic function in the hippocampus [59]. Studies also demonstrate that phenolic compounds such as CGA disaggregate Aβ fibrils, reduce toxicity, and block Aβ oligomerization, suggesting their therapeutic potential in the treatment of AD [32]. This reasoning would explain, at least in part, the neuroprotective effect of CGA.

BDNF is essential for long-term potentiation, contributing to neurogenesis, synaptic plasticity, learning, and memory [68]. Studies have already demonstrated a decrease in BDNF expression in the hippocampus and in temporal and frontal cortical regions in patients with AD [69]. Decreased BDNF is related to decreased CREB activity, as well as Aβ accumulation, Tau hyperphosphorylation, neuroinflammation, and neuronal apoptosis. Our data showed that BDNF immunoreactivity was markedly lower in hippocampus and prefrontal cortex in ICV-STZ group. These results are consistent with other studies that also observed a decrease in BDNF expression in the cortex and hippocampus in the ICV-STZ-induced AD model [70]. Kurowska-Rucińska et al., [71] also found that the ICV-STZ led to a reduction in BDNF-containing cells in the hippocampus (DG and CA1–CA3 areas) as well as in the OB of rats in both age groups [71]. The CGA treatment restored BDNF immunoreactivity in hippocampus and prefrontal cortex with values close to the control group. Although little is known about the direct effects of CGA on BDNF levels, studies have shown that natural compounds such as phenolic compounds are effective in inducing neurogenesis and neuronal differentiation by modulating the levels of this neurotrophin [72]. And both GCA and its metabolite, m-coumaric acid, have been shown to promote hippocampal neurite outgrowth, supporting their role in neuroplasticity [73].

Neuroinflammation occurs early in the progression of AD, even before the formation of plaques and tangles [74]. Glial cell activation is closely related to neuroinflammation and plays a significant role in the pathogenesis of AD, starting in the early stages of mild cognitive impairment and peaking in moderately affected cases [75]. Importantly, the neuroinflammation triggered by the injection of ICV-STZ can also be attributed to dysfunction of the IRS/PI3K/AKT/GSK-3β pathway. Several studies have associated brain inflammation with the dysregulation of this signaling pathway [76]. This process contributes to the accumulation of Aβ and hyperphosphorylation of Tau, resulting in increased neuroinflammation and decreased neuronal viability [77]. The CGA was able to decrease astrocyte activation induced by ICV-STZ in the hippocampus and prefrontal cortex. Supporting our data, a study conducted by Shah et al. [78] showed that CGA reduced GFAP expression in the cortex of mice in a model of permanent focal cerebral ischemia. Furthermore, studies have attributed the neuroprotective effect of CGA to the ability to increase anti-inflammatory cytokines such as IL-4 and IL-13, and decrease pro-inflammatory cytokines such as TNF-α, IL-6, IL-1β, and IFN-γ (Lee et al., 2020). Additionally, CGA is known for positively regulating erythroid-related nuclear factor 2 (Nrf-2), and inhibiting the activity of NF-κB, inducible nitric oxide synthase (iNOS), and cyclooxygenase-2 (COX-2) [34]. An increase in microglial activation was observed in the prefrontal cortex and hippocampus of animals subjected to ICV-STZ. Corroborating our results, Liu et al. [79] observed an increase in the number of positive cells for Iba-1 and GFAP, along with increased expression of Iba-1 and GFAP proteins in the hippocampus of animals subjected to ICV-STZ. Furthermore, the study conducted by Rai et al. [80] also showed an increase in the protein expression of CD11b, a marker of microglia in rats, both in the cortex and hippocampus, indicating glial activation and neuroinflammation. Treatment with CGA was able to decrease the activation of microglia in the prefrontal cortex and hippocampus. Consistent with our findings, Shah et al. [78] showed that treatment with CGA decreased the expression of Iba-1 in the cortex of mice in a model of permanent focal cerebral ischemia. Additionally, research has also shown that CGA reduces the levels of nuclear factor kappa B (NF-κB p65) [81], thus contributing to its anti-inflammatory effect. The NF-κB pathway

is closely related to the body's autoimmunity and plays a key regulatory role in the secretion of pro-inflammatory cytokines, chemokines, and adhesion molecules [82]. Moreover, there is evidence suggesting that CGA may be involved in the tyrosine kinase/signal transducer and transcriptional activator 3 signal pathway and inhibits the expression of the IL-6 receptor β subunit, as well as tyrosine kinase 1 phosphorylation of signal transducer and transcriptional activator 3 under oxidative stress. Miao et al. [83] demonstrated that CGA has a strong effect on arachidonic acid metabolism, inhibiting the activation of inflammatory factors.

Conclusion

In conclusion, this study demonstrates the neuroprotective potential of CGA on memory and neuronal viability, through mechanisms involving decreased oxidative stress and neuroinflammation and increased BDNF expression. Thus, CGA proved to be a promising therapeutic alternative for AD.

Author Contributions Jéssica Rabelo Bezerra: Carrying out the animal protocol, Behavioral Tests and Immunohistochemistry analysis, statistical analysis, results interpretation, discussion, and manuscript preparation.

Tycianne de Sousa Nascimento: Carrying out the animal protocol, Behavioral Tests and Immunohistochemistry analysis.

Juliete Tavares: Carrying out the animal protocol, Behavioral Tests and Immunohistochemistry analysis.

Mayara Sandrielly Soares de Aguiar: Statistical analysis, results interpretation, discussion, and manuscript preparation.

Maiara Virgínia Viana Maia: Results interpretation, discussion, and manuscript preparation.

Geanne Matos de Andrade: Experimental design, statistical analysis, results interpretation, discussion, and manuscript preparation.

Data Availability Supporting data are available from the corresponding author upon reasonable request.

Declarations

Competing Interests The authors have no conflicts of interest to declare.

Ethics approval All procedures in the study followed the ethical principles of animal experimentation established by the National Council for Animal Experimentation Control (CONCEA). The protocol was approved by the Ethics Committee for Animal Use (CEUA—UFC) of the UFC under registration number 8904290319.

Consent to participate Not applicable.

Consent to publish Not applicable.

References

1. Villemagne VL, Doré V, Bourgeat P, Burnham SC, Laws S, Salvado O, Masters CL, Rowe CC (2017) Aβ-amyloid and Tau Imaging in Dementia. Semin Nucl Med 47:75–88. https://doi.org/10.1053/j.semnuclmed.2016.09.006

2. Srivastava S, Ahmad R, Khare SK (2021) Alzheimer's disease and its treatment by different approaches: A review. Eur J Med Chem 15(216):113320. https://doi.org/10.1016/j.ejmech.2021.113320

3. Mishra SK, Singh S, Shukla S, Shukla (2018) Intracerebroventricular streptozotocin impairs adult neurogenesis and cognitive functions via regulating neuroinflammation and insulin signaling in adult rats. Neurochem Int 113:56–68. https://doi.org/10.1016/j.neuint.2017.11.012

4. Gao LJ, Dai Y, Li XQ, Meng S, Zhong ZQ, Xu SJ (2021) Chlorogenic acid enhances autophagy by upregulating lysosomal function to protect against SH-SY5Y cell injury induced by H2O2. Exp Ther Med 21:426. https://doi.org/10.3892/etm.2021.9843

5. Fleming R, Zeisel J, Bennett K (2020) World Alzheimer Report 2020: Design, dignity, dementia: dementia-related design and the built environment Volume II; Alzheimer's Disease International: London, UK, 2020; Available online https://www.alzint.org/u/WorldAlzheimerReport2020Vol2.pdf

6. Sheppard O, Coleman M (2020) Alzheimer's Disease: Etiology, Neuropathology and Pathogenesis. In: Alzheimer's Disease: Drug Discovery. [s.l.] Exon Publications, 1–22

7. Geng G, Luo HM (2014) The research progress of metals correlated to Alzheimer's disease. Yao Xue Xue Bao 49(10):1372–1376

8. Deture MA, Dickson DW (2019) The neuropathological diagnosis of Alzheimer's disease. Mol Neurodeg 14:1–18

9. Spires TL, Hyman BT (2005) Transgenic models of Alzheimer's disease: learning from animals. NeuroRx 2:423–437. https://doi.org/10.1602/neurorx.2.3.423

10. Prasanna P, Rathee S, Rahul V, Mandal D, Chandra Goud MS, Yadav P, Hawthorne S, Sharma A, Gupta PK, Ojha S, Jha NK, Villa C, Jha SK (2021) Microfluidic Platforms to Unravel Mysteries of Alzheimer's Disease: How Far Have We Come? Life (Basel) 11:1022. https://doi.org/10.3390/life11101022

11. Grieb P (2016) Intracerebroventricular Streptozotocin Injections as a Model of Alzheimer's Disease: in Search of a Relevant Mechanism. Mol Neurobiol 53:1741–1752. https://doi.org/10.1007/s12035-015-9132-3

12. Koch G, Spampinato D (2022) Alzheimer disease and neuroplasticity. Handb Clin Neurol 184:473–479. https://doi.org/10.1016/B978-0-12-819410-2.00027-8

13. Leloup C, Arluison M, Lepetit N, Cartier N, Marfaing-Jallat P, Ferré P, Pénicaud L (1994) Glucose transporter 2 (GLUT 2): expression in specific brain nuclei. Brain Res 638:221–226. https://doi.org/10.1016/0006-8993(94)90653-x

14. Agrawal R, Tyagi E, Shukla R, Nath C (2011) Insulin receptor signaling in rat hippocampus: a study in STZ (ICV) induced memory deficit model. Eur Neuropsychopharmacol 21:261–273. https://doi.org/10.1016/j.euroneuro.2010.11.009

15. Hoyer S, Lannert H (2007) Long-term abnormalities in brain glucose/energy metabolism after inhibition of the neuronal insulin receptor: implication of tau-protein. J Neural Transm Suppl 2007:195–202. https://doi.org/10.1007/978-3-211-73574-9_25

16. Salkovic-Petrisic M, Hoyer S (2007) Central insulin resistance as a trigger for sporadic Alzheimer-like pathology: an experimental approach. J Neural Transm Suppl 2007:217–233. https://doi.org/10.1007/978-3-211-73574-9_28

17. Salkovic-Petrisic M, Knezovic A, Hoyer S, Riederer P (2013) What have we learned from the streptozotocin-induced animal model of sporadic Alzheimer's disease, about the therapeutic

strategies in Alzheimer's research. J Neural Transm (Vienna) 120:233–252. https://doi.org/10.1007/s00702-012-0877-9

18. Salkovic-Petrisic M, Tribl F, Schmidt M, Hoyer S (2006) Riederer P (2006) Alzheimer-like changes in protein kinase B and glycogen synthase kinase-3 in rat frontal cortex and hippocampus after damage to the insulin signalling pathway. J Neurochem 96:1005–1015. https://doi.org/10.1111/j.1471-4159.2005.03637.x

19. Kumar R, Jaggi AS, Singh N (2010) Effects of erythropoietin on memory deficits and brain oxidative stress in the mouse models of dementia. Korean J Physiol Pharmacol 14:345–352. https://doi.org/10.4196/kjpp.2010.14.5.345

20. Saxena G, Patro IK, Nath (2011) ICV STZ induced impairment in memory and neuronal mitochondrial function: A protective role of nicotinic receptor. Behav Brain Res 224:50–7. https://doi.org/10.1016/j.bbr.2011.04.0393

21. Park SJ, Kim YH, Nam GH, Choe SH, Lee SR, Kim SU, Kim JS, Sim BW, Song BS, Jeong KJ, Lee Y, Park YI, Lee KM, Huh JW, Chang KT (2015) Quantitative expression analysis of APP pathway and tau phosphorylation-related genes in the ICV STZ-induced non-human primate model of sporadic Alzheimer's disease. Int J Mol Sci 16:2386–2402. https://doi.org/10.3390/ijms16022386

22. Naveed M, Hejazi V, Abbas M, Kamboh AA, Khan GJ, Shumzaid M, Ahmad F, Babazadeh D, FangFang X, Modarresi-Ghazani F, WenHua L, XiaoHui Z (2018) Chlorogenic acid (CGA): A pharmacological review and call for further research. Biomed Pharmacother 97:67–74. https://doi.org/10.1016/j.biopha.2017.10.064

23. Santana-Gálvez J, Cisneros-Zevallos L, Jacobo-Velázquez DA (2017) Chlorogenic Acid: Recent Advances on Its Dual Role as a Food Additive and a Nutraceutical against Metabolic Syndrome. Molecules 22:358. https://doi.org/10.3390/molecules22030358

24. McCarty MF (2005) A chlorogenic acid-induced increase in GLP-1 production may mediate the impact of heavy coffee consumption on diabetes risk. Med Hypotheses 64:848–853. https://doi.org/10.1016/j.mehy.2004.03.037

25. Bagdas D, Ozboluk HY, Cinkilic N, Gurun MS (2014) Antinociceptive effect of chlorogenic acid in rats with painful diabetic neuropathy. J Med Food 17:730–732. https://doi.org/10.1089/jmf.2013.2966

26. Miao M, Xiang L (2020) Pharmacological action and potential targets of chlorogenic acid. Adv Pharmacol 87:71–88. https://doi.org/10.1016/bs.apha.2019.12.002

27. Kato M, Ochiai R, Kozuma K, Sato H, Katsuragi Y (2018) Effect of Chlorogenic Acid Intake on Cognitive Function in the Elderly: A Pilot Study. Evid Based Complement Alternat Med 7(2018):8608497. https://doi.org/10.1155/2018/8608497

28. Saitou K, Ochiai R, Kozuma K, Sato H, Koikeda T, Osaki N, Katsuragi Y (2018) Effect of Chlorogenic Acids on Cognitive Function: A Randomized, Double-Blind. Placebo-Controlled Trial Nutrients 10:1337. https://doi.org/10.3390/nu10101337

29. Ochiai R, Saitou K, Suzukamo C, Osaki N, Asada T (2019) Effect of Chlorogenic Acids on Cognitive Function in Mild Cognitive Impairment: A Randomized Controlled Crossover Trial. J Alzheimers Dis 72:1209–1216. https://doi.org/10.3233/JAD-190757

30. Ishida K, Yamamoto M, Misawa K, Nishimura H, Misawa K, Ota N, Shimotoyodome A (2020) Coffee polyphenols prevent cognitive dysfunction and suppress amyloid β plaques in APP/PS2 transgenic mouse. Neurosci Res 154:35–44. https://doi.org/10.1016/j.neures.2019.05.001

31. Lim DW, Han T, Jung J, Song Y, Um MY, Yoon M, Kim YT, Cho S, Kim IH, Han D, Lee C, Lee J (2018) Chlorogenic Acid from Hawthorn Berry (Crataegus pinnatifida Fruit) Prevents Stress Hormone-Induced Depressive Behavior, through Monoamine Oxidase B-Reactive Oxygen Species Signaling in Hippocampal Astrocytes of Mice. Mol Nutr Food Res 62:e1800029. https://doi.org/10.1002/mnfr.201800029

32. Lee TK, Kang IJ, Kim B, Sim HJ, Kim DW, Ahn JH, Lee JC, Ryoo S, Shin MC, Cho JH, Kim YM, Park JH, Choi SY, Won MH (2020) Experimental Pretreatment with Chlorogenic Acid Prevents Transient Ischemia-Induced Cognitive Decline and Neuronal Damage in the Hippocampus through Anti-Oxidative and Anti-Inflammatory Effects. Molecules 25:3578. https://doi.org/10.3390/molecules25163578

33. Shi M, Sun F, Wang Y, Kang J, Zhang S, Li H (2020) CGA restrains the apoptosis of Aβ25-35-induced hippocampal neurons. Int J Neurosci 130:700–707. https://doi.org/10.1080/00207454.2019.1702547

34. Paxions G, Franklin KB (2004) The mouse brain in stereotaxic coordinates. Gulf Professional Publishing

35. Lannert H, Hoyer S (1998) Intracerebroventricular administration of streptozotocin causes long-term diminutions in learning and memory abilities and in cerebral energy metabolism in adult rats. Behav Neurosci 112:1199–1208. https://doi.org/10.1037/0735-7044.112.5.1199

36. Sharma M, Gupta YK (2001) Intracerebroventricular injection of streptozotocin in rats produces both oxidative stress in the brain and cognitive impairment. Life Sci 68:1021–1029. https://doi.org/10.1016/s0024-3205(00)01005-5

37. Stefanello N, Schmatz R, Pereira LB, Rubin MA, da Rocha JB, Facco G, Pereira ME, Mazzanti CM, Passamonti S, Rodrigues MV, Carvalho FB, da Rosa MM, Gutierres JM, Cardoso AM, Morsch VM, Schetinger MR (2014) Effects of chlorogenic acid, caffeine, and coffee on behavioral and biochemical parameters of diabetic rats. Mol Cell Biochem 388(1–2):277–286. https://doi.org/10.1007/s11010-013-1919-9

38. Tabák AG, Herder C, Rathmann W, Brunner EJ, Kivimäki M (2012) Prediabetes: a high-risk state for diabetes development. Lancet 379:2279–2290. https://doi.org/10.1016/S0140-6736(12)60283-9

39. Broadhurst PL (1957) Determinants of emotionality in the rat. I Situational factors. Br J Psychol 48:1–12. https://doi.org/10.1111/j.2044-8295.1957.tb00594.x

40. Sarter M, Bodewitz G, Stephens DN (1988) Attenuation of scopolamine-induced impairment of spontaneous alteration behaviour by antagonist but not inverse agonist and agonist beta-carbolines. Psychopharmacology 94:491–495. https://doi.org/10.1007/BF00212843

41. Ennaceur A, Delacour J (1988) A new one-trial test for neurobiological studies of memory in rats. 1: Behavioral data. Behav Brain Res 31(1):47–59. https://doi.org/10.1016/0166-4328(88)90157-x

42. DeNoble VJ, Repetti SJ, Gelpke LW, Wood LM, Keim KL (1986) Vinpocetine: nootropic effects on scopolamine-induced and hypoxia-induced retrieval deficits of a step-through passive avoidance response in rats. Pharmacol Biochem Behav 24:1123–1128. https://doi.org/10.1016/0091-3057(86)90465-x

43. Morris R (1984) Developments of a water-maze procedure for studying spatial learning in the rat. J Neurosci Methods 11:47–60. https://doi.org/10.1016/0165-0270(84)90007-4

44. Draper HH, Hadley M (1990) Malondialdehyde determination as index of lipid peroxidation. Methods Enzymol 186:421–431. https://doi.org/10.1016/0076-6879(90)86135-i

45. Green LC, Wagner DA, Glogowski J, Skipper PL, Wishnok JS, Tannenbaum SR (1982) Analysis of nitrate, nitrite, and [15N] nitrate in biological fluids. Anal Biochem 126:131–138. https://doi.org/10.1016/0003-2697(82)90118-x

46. Scorza CA, Araujo BH, Leite LA, Torres LB, Otalora LF, Oliveira MS, Garrido-Sanabria ER, Cavalheiro EA (2011) Morphological and electrophysiological properties of pyramidal-like neurons in the stratum oriens of Cornu ammonis 1 and Cornu ammonis 2 area of Proechimys. Neuroscience 177:252–268. https://doi.org/10.1016/j.neuroscience.2010.12.054

47. Pacheco SM, Soares MSP, Gutierres JM, Gerzson MFB, Carvalho FB, Azambuja JH, Schetinger MRC, Stefanello FM, Spanevello RM (2018) Anthocyanins as a potential pharmacological agent to manage memory deficit, oxidative stress and alterations in ion pump activity induced by experimental sporadic dementia of Alzheimer's type. J Nutr Biochem 56:193–204. https://doi.org/10.1016/j.jnutbio.2018.02.014

48. Fernandes MYD, Dobrachinski F, Silva HB, Lopes JP, Gonçalves FQ, Soares FAA, Porciúncula LO, Andrade GM, Cunha RA, Tomé AR (2021) Neuromodulation and neuroprotective effects of chlorogenic acids in excitatory synapses of mouse hippocampal slices. Sci Rep 11:10488. https://doi.org/10.1038/s41598-021-89964-0

49. Roy A, Sharma S, Nag TC, Katyal J, Gupta YK, Jain S (2022) Cognitive Dysfunction and Anxiety Resulting from Synaptic Downscaling, Hippocampal Atrophy, and Ventricular Enlargement with Intracerebroventricular Streptozotocin Injection in Male Wistar Rats. Neurotox Res 40:2179–2202. https://doi.org/10.1007/s12640-022-00563-x

50. Rostami F, Javan M, Moghimi A, Haddad-Mashadrizeh A, Fereidoni M (2017) Streptozotocin-induced hippocampal astrogliosis and insulin signaling malfunction as experimental scales for subclinical sporadic Alzheimer model. Life Sci 188:172–185. https://doi.org/10.1016/j.lfs.2017.08.025

51. Gáspár A, Hutka B, Ernyey AJ, Tajti BT, Varga BT, Zádori ZS, Gyertyán I (2021) Intracerebroventricularly Injected Streptozotocin Exerts Subtle Effects on the Cognitive Performance of Long-Evans Rats. Front Pharmacol 12:662173. https://doi.org/10.3389/fphar.2021.662173

52. Fischer R, Maier O (2015) Interrelation of oxidative stress and inflammation in neurodegenerative disease: role of TNF. Oxid Med Cell Longev 2015:610813. https://doi.org/10.1155/2015/610813

53. Kim GH, Kim JE, Rhie SJ, Yoon S (2015) The Role of Oxidative Stress in Neurodegenerative Diseases. Exp Neurobiol 24:325–340. https://doi.org/10.5607/en.2015.24.4.325

54. Huang WJ, Zhang X, Chen WW (2016) Role of oxidative stress in Alzheimer's disease. Biomed Rep 4:519–522. https://doi.org/10.3892/br.2016.630

55. Nazem A, Sankowski R, Bacher M, Al-Abed Y (2015) Rodent models of neuroinflammation for Alzheimer's disease. J Neuroinflammation 17(12):74. https://doi.org/10.1186/s12974-015-0291-y

56. Rajasekar N, Dwivedi S, Nath C, Hanif K, Shukla R (2014) Protection of streptozotocin induced insulin receptor dysfunction, neuroinflammation and amyloidogenesis in astrocytes by insulin. Neuropharmacology 86:337–352. https://doi.org/10.1016/j.neuropharm.2014.08.013

57. Ishrat T, Khan MB, Hoda MN, Yousuf S, Ahmad M, Ansari MA, Ahmad AS, Islam F (2006) Coenzyme Q10 modulates cognitive impairment against intracerebroventricular injection of streptozotocin in rats. Behav Brain Res 171(1):9–16. https://doi.org/10.1016/j.bbr.2006.03.009

58. Kwon SH, Lee HK, Kim JA, Hong SI, Kim HC, Jo TH, Park YI, Lee CK, Kim YB, Lee SY, Jang CG (2010) Neuroprotective effects of chlorogenic acid on scopolamine-induced amnesia via anti-acetylcholinesterase and anti-oxidative activities in mice. Eur J Pharmacol 649:210–217. https://doi.org/10.1016/j.ejphar.2010.09.001

59. Gao L, Li X, Meng S, Ma T, Wan L, Xu S (2020) Chlorogenic Acid Alleviates Aβ25-35-Induced Autophagy and Cognitive Impairment via the mTOR/TFEB Signaling Pathway. Drug Des Devel Ther 14:1705–1716. https://doi.org/10.2147/DDDT.S235969

60. Natella F, Nardini M, Di Felice M, Scaccini C (1999) Benzoic and cinnamic acid derivatives as antioxidants: structure-activity relation. J Agric Food Chem 47:1453–1459. https://doi.org/10.1021/jf980737w

61. Cleary JP, Walsh DM, Hofmeister JJ, Shankar GM, Kuskowski MA, Selkoe DJ, Ashe KH (2005) Natural oligomers of the amyloid-beta protein specifically disrupt cognitive function. Nat Neurosci 8:79–84. https://doi.org/10.1038/nn1372

62. Shanmuganathan B, Sheeja Malar D, Sathya S, Pandima Devi K (2015) Antiaggregation Potential of Padina gymnospora against the Toxic Alzheimer's Beta-Amyloid Peptide 25–35 and Cholinesterase Inhibitory Property of Its Bioactive Compounds. PLoS ONE 10:e0141708. https://doi.org/10.1371/journal.pone.0141708

63. Shanmuganathan B, Suryanarayanan V, Sathya S, Narenkumar M, Singh SK, Ruckmani K, Pandima Devi K (2018) Anti-amyloidogenic and anti-apoptotic effect of α-bisabolol against Aβ induced neurotoxicity in PC12 cells. Eur J Med Chem 143:1196–1207. https://doi.org/10.1016/j.ejmech.2017.10.017

64. Hong-Qi Y, Zhi-Kun S, Sheng-Di C (2012) Current advances in the treatment of Alzheimer's disease: focused on considerations targeting Aβ and tau. Transl Neurodegener 1:21. https://doi.org/10.1186/2047-9158-1-21

65. Knezovic A, Osmanovic-Barilar J, Curlin M, Hof PR, Simic G, Riederer P, Salkovic-Petrisic M (2015) Staging of cognitive deficits and neuropathological and ultrastructural changes in streptozotocin-induced rat model of Alzheimer's disease. J Neural Transm (Vienna) 122:577–592. https://doi.org/10.1007/s00702-015-1394-4

66. Ravelli KG, Rosário BD, Camarini R, Hernandes MS, Britto LR (2017) Intracerebroventricular Streptozotocin as a Model of Alzheimer's Disease: Neurochemical and Behavioral Characterization in Mice. Neurotox Res 31:327–333. https://doi.org/10.1007/s12640-016-9684-7

67. Szkudelski T (2001) The mechanism of alloxan and streptozotocin action in B cells of the rat pancreas. Physiol Res 50:537–546 (**PMID: 11829314**)

68. Tapia-Arancibia L, Aliaga E, Silhol M, Arancibia S (2008) New insights into brain BDNF function in normal aging and Alzheimer disease. Brain Res Rev 59:201–220. https://doi.org/10.1016/j.brainresrev.2008.07.007

69. Gamba P, Staurenghi E, Testa G, Giannelli S, Sottero B, Leonarduzzi G (2019) A Crosstalk Between Brain Cholesterol Oxidation and Glucose Metabolism in Alzheimer's Disease. Front Neurosci 13:556. https://doi.org/10.3389/fnins.2019.00556. (**zhao31**)

70. Zhao HL, Cui SY, Qin Y, Liu YT, Cui XY, Hu X, Kurban N, Li MY, Li ZH, Xu J, Zhang YH (2021) Prophylactic effects of sporoderm-removed Ganoderma lucidum spores in a rat model of streptozotocin-induced sporadic Alzheimer's disease. J Ethnopharmacol 269:113725. https://doi.org/10.1016/j.jep.2020.113725

71. Kurowska-Rucińska E, Ruciński J, Myślińska D, Grembecka B, Wrona D, Majkutewicz I (2022) Dimethyl Fumarate Alleviates Adult Neurogenesis Disruption in Hippocampus and Olfactory Bulb and Spatial Cognitive Deficits Induced by Intracerebroventricular Streptozotocin Injection in Young and Aged Rats. Int J Mol Sci 23:15449. https://doi.org/10.3390/ijms232415449

72. An J, Chen B, Tian D, Guo Y, Yan X, Yang H (2022) Regulation of Neurogenesis and Neuronal Differentiation by Natural Compounds. Curr Stem Cell Res Ther 17:756–771. https://doi.org/10.2174/1574888X16666210907141447

73. Ito H, Sun XL, Watanabe M, Okamoto M, Hatano T (2008) Chlorogenic acid and its metabolite m-coumaric acid evoke neurite outgrowth in hippocampal neuronal cells. Biosci Biotechnol Biochem 72:885–888. https://doi.org/10.1271/bbb.70670

74. Kamat PK, Tota S, Rai S, Swarnkar S, Shukla R, Nath C (2012) A study on neuroinflammatory marker in brain areas of okadaic acid (ICV) induced memory impaired rats. Life Sci 90(19–20):713–720. https://doi.org/10.1016/j.lfs.2012.03.012

75. Ifuku M, Katafuchi T, Mawatari S, Noda M, Miake K, Sugiyama M, Fujino T (2012) Anti-inflammatory/anti-amyloidogenic effects of plasmalogens in lipopolysaccharide-induced neuroinflammation in adult mice. J Neuroinflammation 9:197. https://doi.org/10.1186/1742-2094-9-197

76. Gerzson MFB, Bona NP, Soares MSP, Teixeira FC, Rahmeier FL, Carvalho FB, da Cruz FM, Onzi G, Lenz G, Gonçales RA, Spanevello RM, Stefanello FM (2020) Tannic Acid Ameliorates STZ-Induced Alzheimer's Disease-Like Impairment of Memory, Neuroinflammation, Neuronal Death and Modulates Akt Expression. Neurotox Res 37:1009–1017. https://doi.org/10.1007/s12640-020-00167-3

77. Kamat PK (2015) Streptozotocin induced Alzheimer's disease like changes and the underlying neural degeneration and regeneration mechanism. Neural Regen Res 10:1050–1052. https://doi.org/10.4103/1673-5374.160076

78. Shah MA, Kang JB, Park DJ, Kim MO, Koh PO (2022) Chlorogenic acid alleviates cerebral ischemia-induced neuroinflammation via attenuating nuclear factor kappa B activation. Neurosci Lett 773:136495. https://doi.org/10.1016/j.neulet.2022.136495

79. Liu S, Fan M, Xu JX, Yang LJ, Qi CC, Xia QR, Ge JF (2022) Exosomes derived from bone-marrow mesenchymal stem cells alleviate cognitive decline in AD-like mice by improving BDNF-related neuropathology. J Neuroinflammation 19:35. https://doi.org/10.1186/s12974-022-02393-2

80. Rai S, Kamat PK, Nath C, Shukla R (2014) Glial activation and post-synaptic neurotoxicity: the key events in Streptozotocin (ICV) induced memory impairment in rats. Pharmacol Biochem Behav 117:104–117. https://doi.org/10.1016/j.pbb.2013.11.035

81. Guo YJ, Luo T, Wu F, Mei YW, Peng J, Liu H, Li HR, Zhang SL, Dong JH, Fang Y, Zhao L (2015) Involvement of TLR2 and TLR9 in the anti-inflammatory effects of chlorogenic acid in HSV-1-infected microglia. Life Sci 127:12–18. https://doi.org/10.1016/j.lfs.2015.01.036

82. Ruifeng G, Yunhe F, Zhengkai W, Ershun Z, Yimeng L, Minjun Y, Xiaojing S, Zhengtao Y, Naisheng Z (2014) Chlorogenic acid attenuates lipopolysaccharide-induced mice mastitis by suppressing TLR4-mediated NF-κB signaling pathway. Eur J Pharmacol 729:54–58. https://doi.org/10.1016/j.ejphar.2014.01.015

83. Miao M, Cao L, Li R, Fang X, Miao Y (2017) Protective effect of chlorogenic acid on the focal cerebral ischemia reperfusion rat models. Saudi Pharm J 25:556–563. https://doi.org/10.1016/j.jsps.2017.04.023